CrystEngComm

Accepted Manuscript

ROYAL SOCIETY OF CHEMISTRY

www.rsc.org/crystengcomm

1,2,4,5-Benzenetetrasulfonic acid and 1,4-Benzenedisulfonic acid as sulfo analogues of pyromellitic and terephthalic acid for building coordination polymers of manganese

Christina Zitzer[a], Thomas W. T. Muesmann[a], Jens Christoffers[a], Christian Schwickert[b], Rainer Pöttgen[b] and Mathias S. Wickleder*[a]

* Corresponding Author
Fax: +49 (441) 798 3352
E-Mail: mathias.wickleder@uni-oldenburg.de

[a] MSc. Christina Zitzer, Dr. Thomas W. T. Muesmann, Prof. Dr. Jens Christoffers, Prof. Dr. M. S. Wickleder,
Carl von Ossietzky Universität Oldenburg
Institut für Chemie
Carl-von-Ossietzky-Strasse 9-11
26129 Oldenburg, Germany

[b] Dipl.-Chem. Christian Schwickert, Prof. Dr. Rainer Pöttgen
Westfälische Wilhelms-Universität Münster
Institut für Anorganische und Analytische Chemie
Corrensstraße 30
48149 Münster, Germany

Keywords. Manganese; polysulfonic acids; coordination polymers; crystal structure; thermal behavior; magnetism

Abstract

The new polysulfonic acids H_4B4S (1,2,4,5-benzenetetrasulfonic acid) and H_2BDS (1,4-benzenedisulfonic acid) were used for the preparation of five manganese coordination polymers. The reactions of H_4B4S and $MnCO_3$ were performed in dimethylformamide (DMF) or *N*-methylpyrrolidone (NMP) as solvents in sealed glass ampoules at elevated temperatures. Two benzenetetrasulfonates could be obtained, $[NH_2(CH_3)_2]_2\{Mn(B4S)(DMF)_2\}$ (**I**) ($P2_1/c$, $Z = 2$, $a = 942.02(5)$ pm, $b = 1684.86(6)$ pm, $c = 918.45(5)$ pm, $\beta = 97.746(6)°$, R_1; wR_2 ($I_o > 2\sigma(I_o)$) = 0.0357; 0.0771) and $[HNMP]_2\{Mn(B4S)(NMP)_2\}$ (**II**) ($P2_1/c$, $Z = 2$, $a = 931.7(1)$ pm, $b = 1049.2(1)$ pm, $c = 1944.9(1)$ pm, $\beta = 113.529(3)°$, R_1; wR_2 ($I_o > 2\sigma(I_o)$) = 0.0470; 0.0952). Both compounds exhibit anionic chains according to $_\infty^1\{Mn(B4S)_{2/2}(L)_2\}^{2-}$ (L = DMF, NMP). The Mn^{2+} ions are in octahedral coordination of oxygen atoms. The charge of the anionic chains is either compensated by dimethylammonium cations, $[NH_2(CH_3)_2^+]$ or by protonated NMP molecules, $HNMP^+$. Solvothermal reactions of H_2BDS and $MnCO_3$ in the solvents DMF, NMP and dimethylacetamide (DMA), respectively, yielded the disulfonates $Mn(BDS)(DMF)_2$ (**III**) (*P*-1, $Z = 1$, $a = 514.3(1)$ pm, $b = 926.2(1)$ pm, $c = 940.2(1)$ pm, $\alpha =$

93.552(8)°, β = 99.993(7)°, γ = 99.237(7)°, R_1; wR_2 ($I_o > 2\sigma(I_o)$) = 0.0290; 0.0637), Mn(BDS)(DMA)$_2$ (**IV**) (*P*-1, *Z* = 2, *a* = 936.00(4) pm, *b* = 984.94(4) pm, *c* = 1034.75(5) pm, α = 81.606(2)°, β = 88.941(2)°, γ = 82.364(2)°, R_1; wR_2 ($I_o > 2\sigma(I_o)$) = 0.0387; 0.1046) and Mn(BDS)(NMP)$_2$ (**V**) (*P*-1, *Z* = 2, *a* = 962.97(3) pm, *b* = 976.76(3) pm, *c* = 1034.23(3) pm, α = 89.371(1)°, β = 78.839(1)°, γ = 87.604(2)°, R_1; wR_2 ($I_o > 2\sigma(I_o)$) = 0.0243; 0.0713). In the crystal structures of the three compounds the octahedrally coordinated Mn^{2+} ions are linked by the disulfonate ions to layers according to $^2_\infty${Mn(BDS)$_{4/4}$(L)$_2$} (L = DMF, DMA, NMP). The thermal analysis of all compounds shows that they can be desolvated completely and that the remaining solvent-free sulfonates exhibit decomposition temperatures up to 500 °C what is exceptionally high when compared to the respective carboxylates. Temperature-dependent magnetic susceptibility measurements of [NH$_2$(CH$_3$)$_2$]$_2${Mn(B*4*S)(DMF)$_2$} show paramagnetic behavior of the Mn^{2+} ions.

Introduction

The connection of metal ions or metal oxo-clusters by polydentate ligands leads to frameworks of various dimensionalities with respect to the linkage. Chain type compounds (1D), layer structures (2D), and complex networks (3D) have been reported.[1,2] They are usually named coordination polymers (CPs) and those compounds with frameworks exhibiting large open pores are referred to as metal-organic frameworks (MOFs).[3] By the choice of the metal that is used for building CPs and MOFs specific properties can be implemented. For example rare earth metals may lead to interesting luminescence properties,[4,5] while transition metals like Mn, Fe, Co and Ni can cause paramagnetism or even cooperative magnetic phenomena.[5-7] The dimensionality and the porosity of CPs and MOFs can be tuned by the choice of the polydentate ligands, the so-called linkers.[8-10] The majority of used linkers are polycarboxylate anions and neutral nitrogen-containing heterocycles. One of the reasons for the extensive use of polycarboxylates is that the respective polycarboxylic acids are commercially available in a great variety or that they at least can be prepared very easily. Unfortunately this is not the case for the sulfo analogues of these acids, the so-called polysulfonic acids. Only a limited number of these acids is available and most of the compounds are even lacking reliable synthesis protocols. On the other hand it has been shown that polysulfonate anions are interesting linkers because they show different coordination chemistry compared to carboxylates. For example polysulfonates are weaker ligands making them good candidates for the formation of very flexible host structures. This has been intensively studied for those polysulfonic acids which are available up to now.[11,12] However, it remained the problem that a lot of potentially interesting polysulfonic acids were not accessible. This was especially true for the analogues of very simple and widely used polycarboxylic acids like 1,4-benzenedicarboxylic acid ("terephthalic acid"), 1,3,5-benzenetricarboxcylic acid ("trimesic acid"), 1,2,4,5-benezene-tetrasulfonic acid ("pyromellitic acid"), and 1,2,3,4,5,6-benzene-hexasulfonic acid ("mellitic acid"). Thus, some years ago, we initiated a research program aiming at the development of simple and scalable preparation routes for polysulfonic acids and their use for the preparation of new CPs and MOFs. In the course of these investigations we were also able to prepare the sulfo analogues of the above mentioned carboxylic acids (Fig. 1).[13-15] It turned out that the metal salts of these acids usually show low-dimensional structures (1D, 2D) with the metals additionally coordinated by solvent molecules. In all cases, however, the solvent can be removed by heating without decomposition of the organic linker. In some cases the desolvated compounds are thermally stable up to 600 °C what is remarkably high, especially when compared to the respective carboxylates. This is of special interest if temperature sensible functions of the desolvated compounds like gas storage are envisioned. As a further result of our ongoing research we here present the new

manganese compounds of 1,4-benzene-disulfonic acid (H_2BDS, **1**) and 1,2,4,5-benzene-tetrasulfonic acid (H_4B4S, **2**).

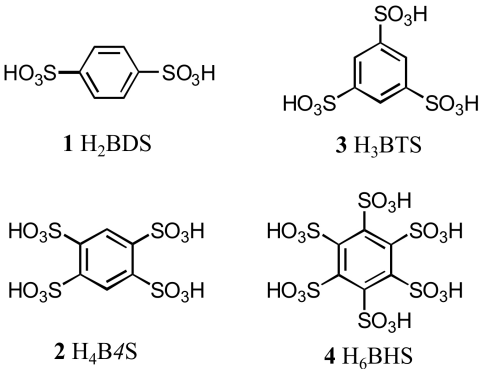

Figure 1. Selected polysulfonic acids which have been prepared in our groups as sulfo analogues of well-known polycarboxylic acids. The manganese salts of **1** and **2** are presented in this work.

Experimental Section

Preparation of Compounds. General. The reactions were carried out in thick walled glass ampoules (length: 300 mm, diameter: 16 mm). The ampoules were loaded with the reactants, torch-sealed under vacuum, and placed in a resistance furnace. The ampoules are heated up to 105 °C within 6 h, hold for 24 h and cooled down to room temperature within 96 h. The products were obtained as colorless crystals which were separated from the supernatant liquid by decantation. **$[NH_2(CH_3)_2]_2\{Mn(B4S)(DMF)_2\}$**: 20 mg (0.043 mmol) H_4B4S, 14 mg (0.122 mmol) $MnCO_3$, 3 ml DMF. **$[HNMP]_2\{Mn(B4S)(NMP)_2\}$**: 20 mg (0.043 mmol) H_4B4S, 5 mg (0.043 mmol) $MnCO_3$, 3 ml NMP. **$Mn(BDS)(DMF)_2$**: 20 mg (0.073 mmol) H_2BDS, 17 mg (0.148 mmol) $MnCO_3$, 3 ml DMF. **$Mn(BDS)(DMA)_2$**: 20 mg (0.073 mmol) H_2BDS, 8 mg (0.070 mmol) $MnCO_3$, 3 ml DMA. **$Mn(BDS)(NMP)_2$**: 20 mg (0.073 mmol) H_2BDS, 17 mg (0.148 mmol) $MnCO_3$, 3 ml NMP. The acids H_2BDS and H_4B4S were prepared as previously described.[13-15] $MnCO_3$ turned out to be the best starting product while the use of manganese acetate or nitrate usually leads to undesired by-products (solvates of the salts). However, even under different reaction conditions the product usually contain traces of $MnCO_3$ that is not seen in XRD but in magnetochemistry.

IR spectroscopy. IR-data were collected with a Bruker Tensor 27 Spectrometer using the ATR-method (attenuated total reflection) on some dried single crystals. The specimen was prepared and placed onto the detector head in a glovebox and transferred to the spectrometer under inert atmosphere. The IR-data were processed with the OPUS 6.5 program.[16]

$[NH_2(CH_3)_2]_2\{Mn(B4S)(DMF)_2\}$: IR(ATR): nu(tilde) = 3471 (w), 3118 (m), 2807 (w), 2451 (w), 1651 (s), 1614 (m), 1465 (m), 1441 (m), 1376 (m), 1309 (w), 1274 (m), 1239 (s), 1183 (s), 1136 (s), 1109 (s), 1041 (s), 937 (m), 892 (m), 856 (m), 828 (m), 686 (s), 669 (m), 644 (s), 573 (m), 546 (s) cm^{-1}. **$[HNMP]_2\{Mn(B4S)(NMP)_2\}$**: 3548 (m), 3461 (w), 3368 (m), 3095 (m), 1656 (s), 1518 (m), 1476 (m), 1459 (m), 1410 (m), 1311 (m), 1240 (s), 1177 (s), 1107 (s), 1045 (s), 1014 (s), 980 (m), 932 (m), 685 (s), 665 (s), 642 (s), 566 (m) cm^{-1}. **$Mn(BDS)(DMF)_2$**: 2992 (w), 2938 (w), 2898 (w), 1652 (s), 1501 (w), 1440 (w), 1415 (m), 1389 (m), 1237 (s), 1184 (s), 1139 (s),

1109 (s), 1050 (s), 1011 (s), 870 (w), 846 (m), 685 (m), 664 (s), 579 (s), 570 (s), 528 (w) cm^{-1}. **$Mn(BDS)(DMA)_2$**: 3542 (m), 3347 (m), 3221 (m), 3097 (w), 1633 (s), 1470 (w), 1393 (m), 1167 (s), 1128 (s), 1109 (s), 1035 (s), 998 (s), 833 (s), 663 (s), 564 (s) 531 (w) cm^{-1}. **$Mn(BDS)(NMP)_2$**: 3551 (m), 3345 (m), 3225 (m), 3097 (w), 1633 (m), 1394 (m), 1169 (s), 1131 (s), 1110 (s), 1042 (s), 1002 (s), 834 (s), 673 (s), 565 (s), 535 (m) cm^{-1}.

X-ray structure determination. Single crystals of the compounds $[HNMP]_2\{Mn(B4S)(NMP)_2\}$, $Mn(BDS)(DMF)_2$, $Mn(BDS)(DMA)_2$, $Mn(BDS)(NMP)_2$ were selected under protecting oil and transferred into the cold nitrogen stream (120 K) of a single-crystal diffractometer (BRUKER APEX II). The crystals of $[NH_2(CH_3)_2]_2\{Mn(B4S)(DMF)_2\}$ are measured at 296 K on a single-crystal diffractometer (Stoe IPDS I). The collection of intensity data was performed at the before mentioned temperature for the respective best specimen. The structure solutions were successful applying Direct Methods and the structures were expanded by Fourier techniques. Refinement of the structures with introduction of anisotropic displacement parameters for all non-hydrogen atoms was performed after the data have been corrected for absorption effects. All calculations were performed with the SHELX program, the data were processed with the programs X-Red and X-Shape.[17] After the refinement of the structure $[HNMP]_2\{Mn(B4S)(NMP)_2\}$ a large electron density remained which could be attributed to the disorder of the $[HNMP]^+$ cation and the SO_3-groups of the benzenetetrasulfonate anions. The disorder was well resolved using split positions for the respective molecules leading an occupancy ratio of 6:4 for the SO_3-groups of the $B4S^{4-}$ anions and 7:3 for the $[HNMP]^+$ cation, and gives a $R_1 = 0.0387$. Also in the compound $Mn(BDS)(DMA)_2$ a disorder of the solvent molecule occurs. The DMA molecule with the numbering O2/C21/C22/N2/C23/C24 has two arrangements. The disorder was well resolved using split positions for the DMA molecules leading an occupancy ratio of 7.5:2.5 and gives a $R_1 = 0.0348$. Table 4 and 5 gives details of the data collection and the obtained crystallographic data. In Table 6 and 7 important distances are summarized.

Thermal analysis. The investigation of the thermal behavior was performed using a TGA/DSC apparatus (Mettler-Toledo GmbH, Schwerzenbach, Switzerland). In a flow of dry oxygen, about 5 mg of the respective compound were placed in a corundum crucible and heated at a rate of 10 K/min up to 1050 °C. The collected data were processed using the software of the analyzer (Mettler-Toledo STARe V9.3).[18] Thermal decomposition data for $[NH_2(CH_3)_2]_2\{Mn(B4S)(DMF)_2\}$, $[HNMP]_2\{Mn(B4S)(NMP)_2\}$, $Mn(BDS)(DMF)_2$, $Mn(BDS)(DMA)_2$ and $Mn(BDS)(NMP)_2$ are presented in Table 2 and Table 3 and Figures 8 and 10.

Powder diffraction. XRD measurements were measured with the help of the powder diffractometer STADIP using Cu-Kα radiation (λ = 154.06 pm). The compounds under investigation were prepared on a flat sample holder. The diffraction data were processed with the WinXPow 2007 program package.[19]

Magnetic property measurements. The magnetic property measurements were carried out using a Quantum Design Physical Property Measurement System using a Vibrating Sample Magnetometer. The measurement was performed in the temperature range of 3-300 K with flux densities up to 80 kOe. 15.569 mg of the polycrystalline sample was packed in a polypropylene capsule and fixed to a brass sample holder rod.

Results and Discussion

Crystal Structures

Benzenetetrasulfonates

The crystal structures of $[NH_2(CH_3)_2]_2\{Mn(B4S)(DMF)_2\}$ (**I**) and $[HNMP]_2\{Mn(B4S)(NMP)_2\}$ (**II**) exhibit anionic chains according to $_\infty^1\{Mn(B4S)_{2/2}(L)_2\}^{2-}$ (L = DMF, NMP). Within the chains both the Mn^{2+} ions and

the centroids of the benzene rings of the anions are located of on special crystallographic positions with -1 site symmetry (Wyckoff sites 2*b* and 2*a*). The Mn^{2+} ions are coordinated by two bidentate B*4*S^{4-} ligands and two solvent molecules (Fig. 2). The resulting [MnO_6] octahedra are quite regular and display distances Mn-O of 217.1(2), 215.4(2) and 216.4(2) pm for compound **I**. The longest bond is found for the coordinating DMF molecules, the shorter ones are those to the B*4*S^{4-} ligands. In **II** the situation is opposite and the shortest distance Mn-O of 215.7(2) pm is that to the NMP molecule while the sulfonate ligands shows slightly larger values of 218.3(3) and 219.1(4) pm, respectively. Another significant difference in the anionic chains of both compounds is the orientation of the [SO_3] moieties of the tetrasulfonates with respect to each other. When viewed along the S·····S direction of neighboring [SO_3] groups it is obvious that the oxygen atoms have a staggered conformation in **I** and an eclipsed one in **II** (Fig. 3).

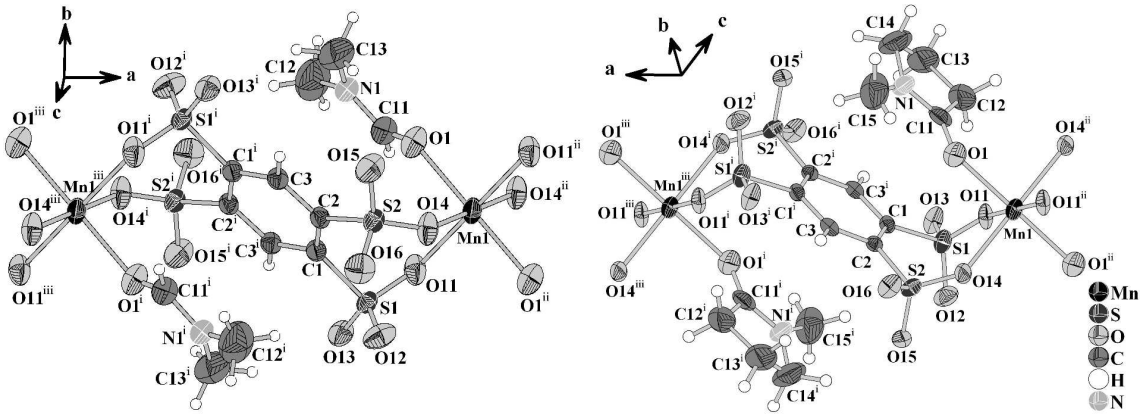

Figure 2. Sections of the anionic chains {Mn(B*4*S)(L)$_2$}$^{2-}$ (L = DMF, NMP) in I (left) and II (right). The Mn atoms and the centroids of the benzene ring are located on special crystallographic sites bearing inversion symmetry. The displacement ellipsoids are drawn at a 50% probability level. Symmetry codes: **I:** (i) = -x, -y, -z; (ii) = 1-x, -y, -z; (iii) = -1+x, y, z; **II:** (i) = -x, -1-y, -1-z; (ii) = -1-x, -1-y, -1-z; (iii) = 1+x, y, z.

The $_\infty^1${Mn(B*4*S)(L)$_2$}$^{2-}$ chains in both compounds are aligned along the [100] direction (Fig. 4). They are arranged in densest rod packing fashion and their charge is compensated by dimethylammonium cations (in **I**) and by protonated NMP molecules (in **II**), respectively. The [$NH_2(CH_3)_2$]$^+$ originate obviously from the partly decomposition of the DMF solvent. The protonation of the NMP molecule can be easily identified by inspection of the C-O distance. It is found at 128.5(6) pm for the [HNMP]$^+$ ion while the respective distance is 123.7(3) pm in the manganese coordinated NMP molecule. Furthermore, the proton can be found in the Fourier map during the crystal structure refinement, even if it was refined by a constrained model. For both of the different cations hydrogen bonds to the non-coordinating oxygen atoms of the [SO_3] group could be identified. In **I** the donor-acceptor distances D-A are found at 283.1(3) and 291.5(3) pm and the angles ∠ DHA are 155(3)° and 160(3)°, hint at medium-strong hydrogen bonds.[20] In compound **II** the hydrogen bonds with donor-acceptor distances of 243.3(4) and 283.8(5) pm with the respective angles ∠ DHA being 136(5)° and 115(4)° (cf. Table 1) are quite strong.[20] The observed hydrogen bonds are emphasized in Fig. 4.

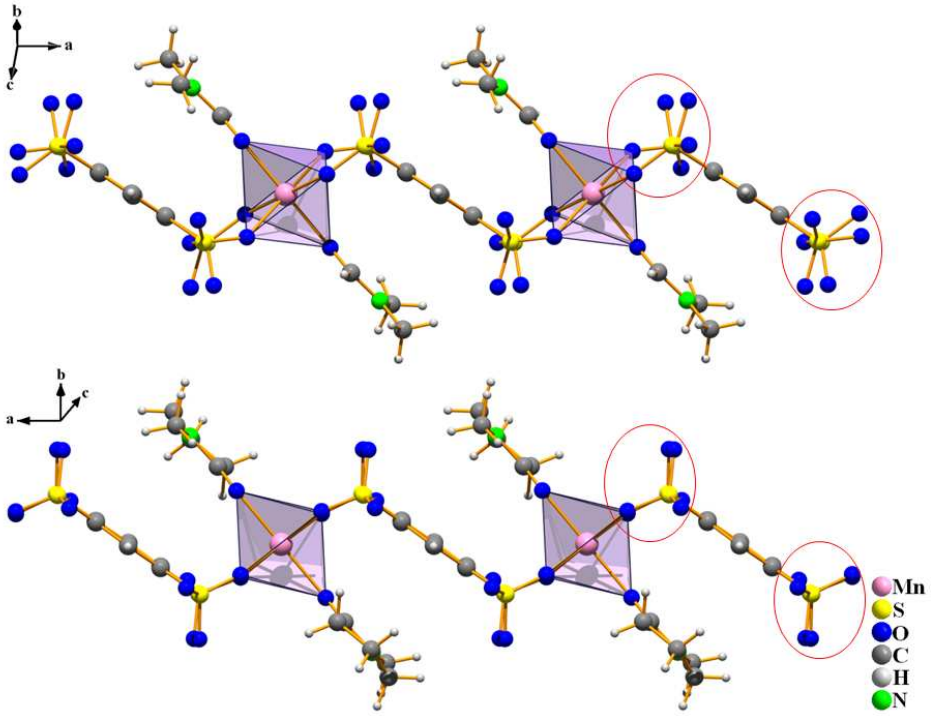

Figure 3. A closer look on the anionic chains in **I** (on top) and **II** (at bottom) shows the differences between the compounds. When viewed along the S·····S direction of neighboring [SO_3] groups the oxygen atoms are either in a staggered (**I**) or ecliptic (**II**) conformation (as emphasized by the red circles).

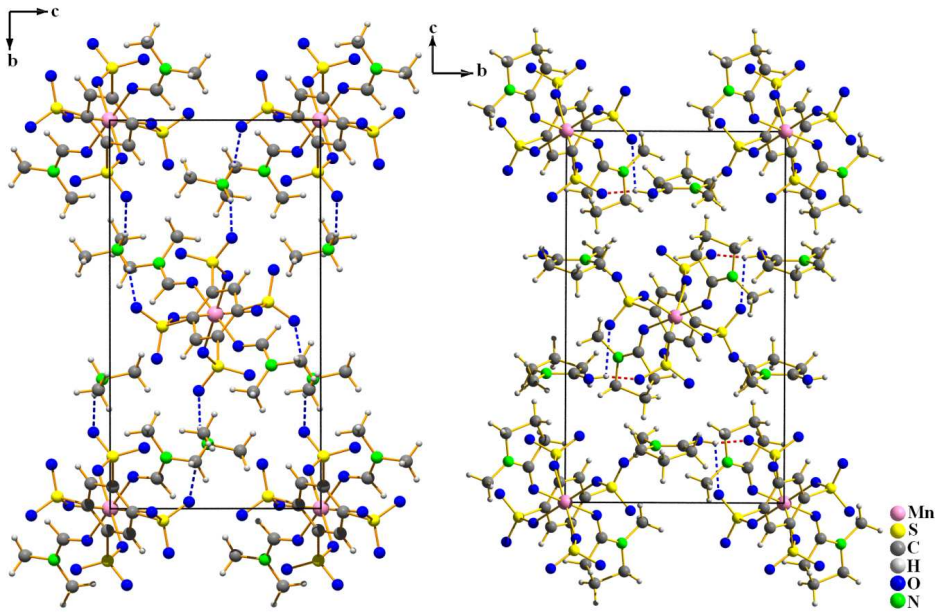

Figure 4. Crystal structures of **I** (left) and **II** (right) viewed along the [100] direction of the monoclinic unit cells. In this direction the anionic chains shown in Fig. 3 are oriented. The charge compensation is achieved by $[NH_2(CH_3)_2]^+$ and $[HNMP]^+$ cations which show also hydrogen bonding to neighboring oxygen atoms of [SO_3] groups. These are emphasized as dashed lines in red (strong H-bonds) and blue (medium strong H-bonds).

Table 1. Hydrogen bonds in $[NH_2(CH_3)_2]_2\{Mn(B4S)(DMF)_2\}$ (**I**) and $[HNMP]_2\{Mn(B4S)(NMP)_2\}$ (**II**) with d(H...A) < r(A) + 200 pm and ∠ DHA > 110 deg. The strong hydrogen bonds are marked in bold.

	D-H	d(D-H)/ pm	d(H···A)/ pm	∠ DHA/ °	d(D···A)/ pm	A
I	N2-H21	93(4)	202(4)	160(3)	291.5(3)	O13^{i}
	N2-H22	100(4)	190(4)	155(3)	283.1(3)	O16
II	**O2-H1**	**85.0(1)**	**175(4)**	**136(5)**	**243.3(4)**	**O15**^{ii}
	O2-H1	85.0(1)	237(5)	115(4)	283.8(5)	O12^{ii}

Symmetry codes: (i) = x, -1/2-y, 1/2+z; (ii) = 1+x, -3/2-y, 1/2+z

Benzenedisulfonates

The manganese benzenedisulfonates $Mn(BDS)(DMF)_2$ (**III**), $Mn(BDS)(DMA)_2$ (**IV**), and $Mn(BDS)(NMP)_2$ (**V**) crystallize with triclinic symmetry. The structures are similar in the way that the Mn^{2+} ions are octahedrally coordinated by oxygen atoms that belong to four disulfonate ligands and two solvent molecules (Fig. 5). The solvent molecules are in *trans* orientation with respect to each other at the apices of the $[MnO_6]$ octahedra. In **III** the $[MnO_6]$ octahedron bears inversion symmetry, i.e. the Mn^{2+} ion is located on a special site of the triclinic unit cell (*Wyckoff* position 1*g*). In **IV** and **V** the manganese atoms are situated on general sites (*Wyckoff* positions 2*i*). In all of the three compounds the distances Mn-O lie in a narrow range between 213 and 219 pm (Table 7).

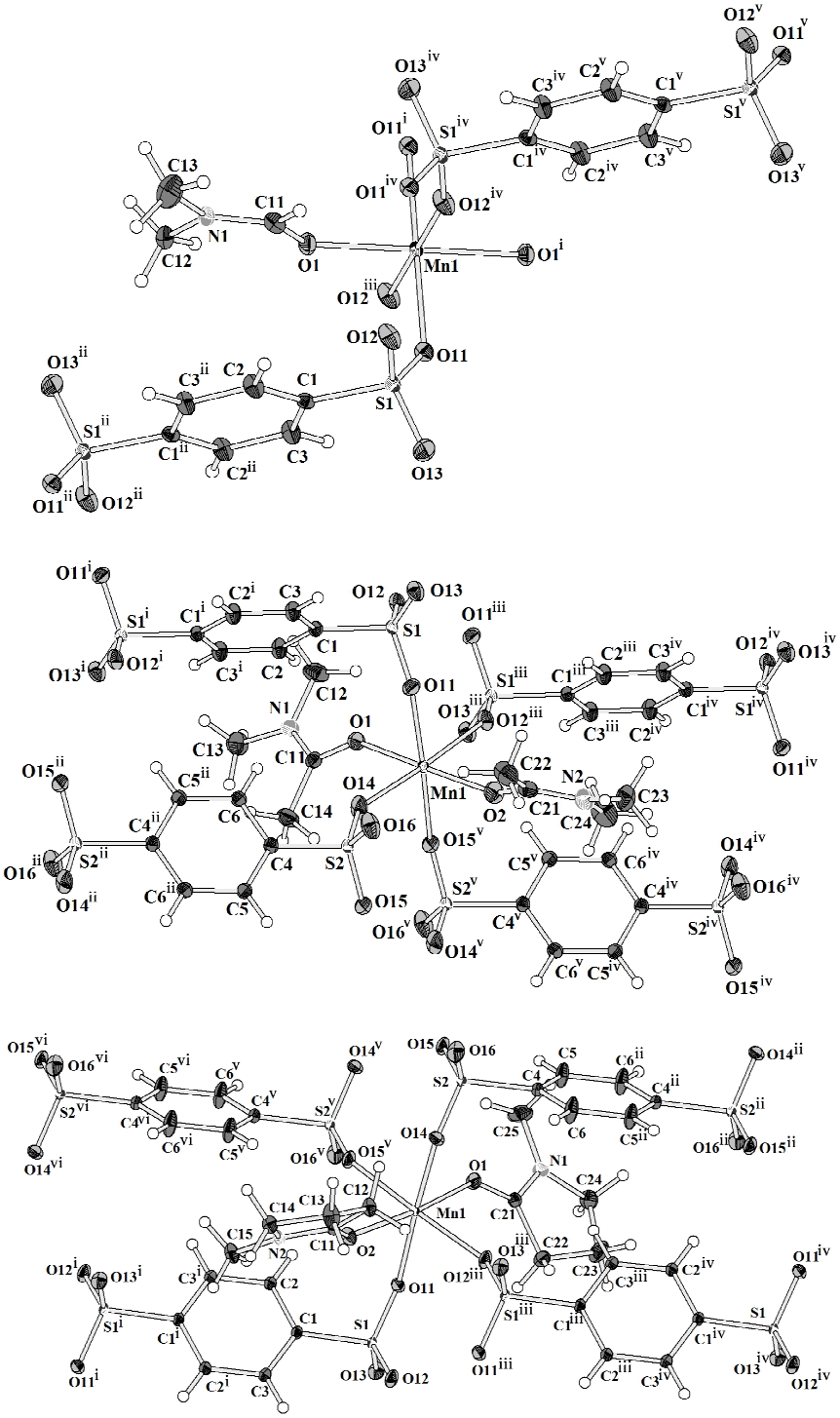

Figure 5. Coordination of the Mn^{2+} ions in $Mn(BDS)(DMF)_2$ (**III**, on top), $Mn(BDS)(DMA)_2$ (**IV**, middle), and $Mn(BDS)(NMP)_2$ (**V**, at bottom). Note that in the structure of **III** the manganese site show inversion symmetry. The displacement ellipsoids are drawn at a 50% probability level. For compound **IV** and **V** the asymmetric unit has two half BDS^{2-} moieties, each lying at independent inversion centres. Symmetry codes: **III**: (i) = -x, 1-y, 1-z; (ii) = 1-x, 2-y, 1-z; (iii) = -1+x, y, z; (iv) = 1-x, 1-y, 1-z; (v) = x, -1+y, z; **IV**: (i) = 1-x, 1-y, 1-z; (ii) = 1-x, 1-y, 2-z; (iii) = 1-x, -y, 1-z; (iv) = x, -1+y, z; (v) = 1-x, -y, 2-z; **V**: (i) = -x, -y, 2-z; (ii) = 2-x, -y, 1-z; (iii) = 1-x, -y, 2-z; (iv) = 1+x, y, z; (v) = 1-x, -y, 1-z; (vi) = -1+x, y, z.

In all of the three compounds the Mn^{2+} ions are linked by the benzenedisulfonate ligands to layers according to $_{\infty}^{2}\{Mn(BDS)_{4/2}(L)_{2/1}\}$ (L = DMF, DMA, NMP) (Fig. 6). The structural differences arise from the arrangement of the BDS^{2-} anions with respect to each other in the individual structures. In **III** the benzenedisulfonate anions have the same orientation while in **IV** and **V** the single BDS^{2-} anions are twisted with respect to each other (Fig. 6). The solvent molecules L point into the interlayer spacing and weak interactions to the non-coordinating oxygen atoms of the $[SO_3]$ moieties of adjacent layers can be assumed.

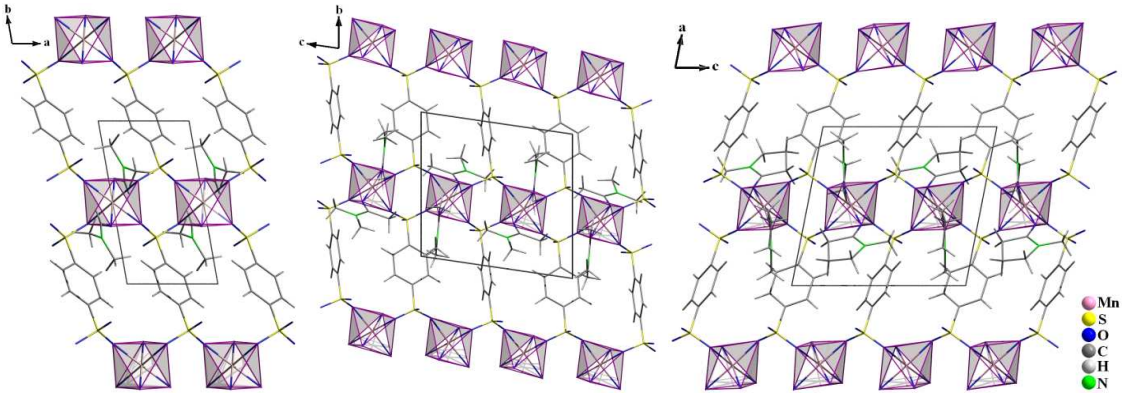

Figure 6. Crystal structures of $Mn(BDS)(DMF)_2$ (**III**, left), $Mn(BDS)(DMA)_2$ (**IV**, middle) and $Mn(BDS)(NMP)_2$ (**V**, right). For all structures the view is onto the $_{\infty}^{2}\{Mn(BDS)_{4/2}(L)_{2/1}\}$ layers. The structures differ due to the different orientation of the BDS^{2-} anions with respect to each other.

Thermal Behaviour

*Thermal decomposition of **I** and **II***

The thermal decomposition of $[NH_2(CH_3)_2]_2\{Mn(B4S)(DMF)_2\}$ (**I**) and $[HNMP]_2\{Mn(B4S)(NMP)_2\}$ (**II**) was monitored by means of DSC/TG measurements in a flow of dry oxygen (Fig. 7, Table 2). Both compounds decompose in multi-step processes; however, these steps are not clearly resolved in any case. Nevertheless it seems clear that the first endothermic steps can be attributed to the loss of the two solvent molecules and the decomposition of the cations under release of $NHMe_2$ for compound **I** and NMP for compound **II**, respectively. This is in good accordance with the observed mass loss of 33 % (calcd. 33 %) for **I** and 47 % (calcd. 46 %) for **II** (cf. Table 2). In both cases this should lead formally to the formation of the dihydrogentetrasulfonate "$Mn(H_2B4S)$", which subsequently decomposes in the course of three exothermic steps. According to XRD investigations at 650°C (compound **I**) and 600 °C (compound **II**), respectively, the decomposition leads to a mixture of $MnSO_4$ and Mn_3O_4 (Fig. 8).[21,22] For **I** also small amounts of MnO_2 are observed in the diffraction pattern.[23] In a final step the manganese(II)sulfate decomposes to Mn_2O_3 according to the XRD pattern of the final residue.[24]

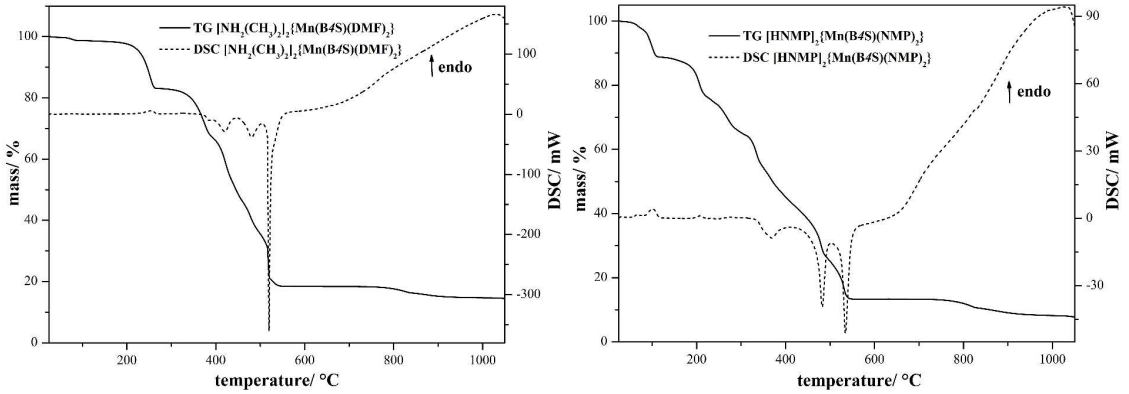

Figure 7. DSC/TG diagrams of the thermal decompositions of $[NH_2(CH_3)_2]_2\{Mn(B4S)(DMF)_2\}$ (**I**) and $[HNMP]_2\{Mn(B4S)(NMP)_2\}$ (**II**). The decompositions are composed of endothermic steps which can be attributed to the loss of solvent molecules and decompositions of the cations $[NH_2(CH_3)_2]^+$ and $[HNMP]^+$, respectively. Subsequently the intermediate product, most probably $Mn(H_2B4S)$ decomposes in various exothermic steps, leading finally to Mn_2O_3 and Mn_3O_4.

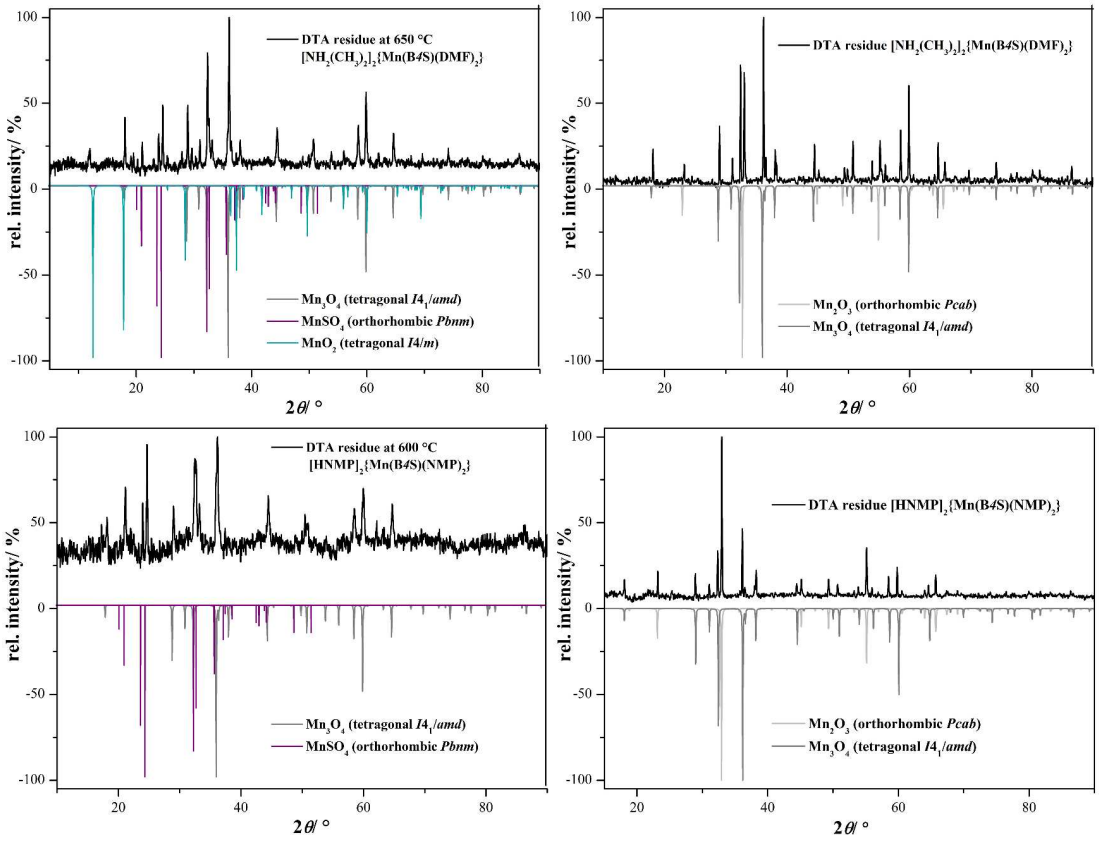

Figure 8. Powder patterns of the intermediates (left) and final decomposition products (right) of **I** (on top) and **II** (at bottom).

Table 2. Thermal decomposition data of the anionic chain compounds **I** and **II**

Stage	T_{onset}/ °C	T_{end}/ °C	T_{max}/ °C	Mass loss obsd./ %	Mass loss calcd./ %	elimination/ decomposition
$[NH_2(CH_3)_2]_2\{Mn(B4S)(DMF)_2\}$ (**I**)						
1	40	85	79	2	33	loss of two equiv. of $NH(CH_3)_2$ and two equiv. of DMF
2	214	270	260	15		
3	326	392	375	16		
4	392	442	420	21	-	decomposition to Mn_3O_4 and $MnSO_4$ and MnO_2
5	455	512	480	10		
6	512	550	520	18		
7	770	845	830	4	-	decomposition to Mn_2O_3 and 4 Mn_3O_4 (calcd. 11%)
∑				86	89	
$[HNMP]_2\{Mn(B4S)(NMP)_2\}$ (**II**)						
1	51	108	65; 100	11	23	loss of two equiv. of NMP
2	185	225	208	13		
3	225	300	235; 268	12	23	loss of two equiv. of NMP
4	308	352	335	11		
5	152	400	370	11	-	decomposition to Mn_3O_4 and $MnSO_4$
6	466	500	484	17		
7	506	550	535	12		
8	720	830	826	5	-	decomposition to Mn_2O_3 and Mn_3O_4 (calcd. 9%)
∑				92	91	

*Thermal decomposition of **III**, **IV**, and **V***

The thermal decomposition of the compounds **III**, **IV**, and **V** was investigated by DSC/TG measurements in a flow of dry oxygen (Fig. 9, Table 3). All of the compounds decompose in three-step processes. The first steps are endothermic and can be attributed to the loss of the solvent molecules. The solvent free manganese benzenedisulfonates Mn(BDS) show high thermal stabilities and the decompositions start clearly above 500 °C. These decompositions lead in a first step to $MnSO_4$ (for **IV** also a small amount of Mn_3O_4 is seen, cf. Fig. 10).[22,23,26] The anhydrous manganese sulfate occurs in two different modifications, as can be seen from XRD measurements of the decomposition products obtained at 650 °C (Fig. 10). As a result of the preparation of the sample on a flat sample holder also reflections of the hydrate $Mn(SO_4)\cdot 2H_2O$ might occur.[27] In any case the manganese sulfate decomposes further leading essentially to Mn_3O_4, although in the case of compound **II** also Mn_2O_3 is found as a minor decomposition product (Fig. 10).[23,25] The quantification of the crystalline phases contained in powder samples of the final product was estimated with respect to the reflection intensities as extracted by determined by Rietveld refinements.[26]

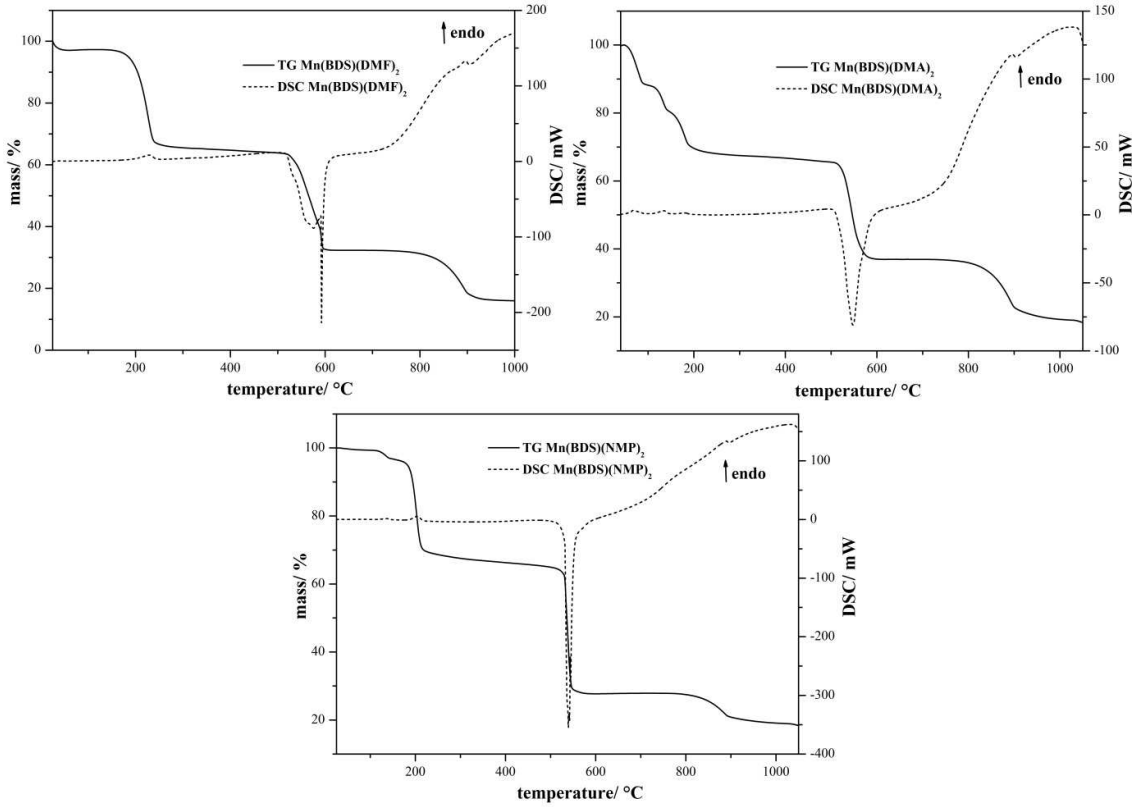

Figure 9. TG/DSC diagram of the thermal decomposition of $Mn(BDS)(DMF)_2$ (**III**), $Mn(BDS)(DMA)_2$ (**IV**), and $Mn(BDS)(NMP)_2$ (**V**). The decomposition of all compounds starts with the loss of the solvent molecules. Finally the solvent-free compounds decompose exothermally at temperatures above 500 °C.

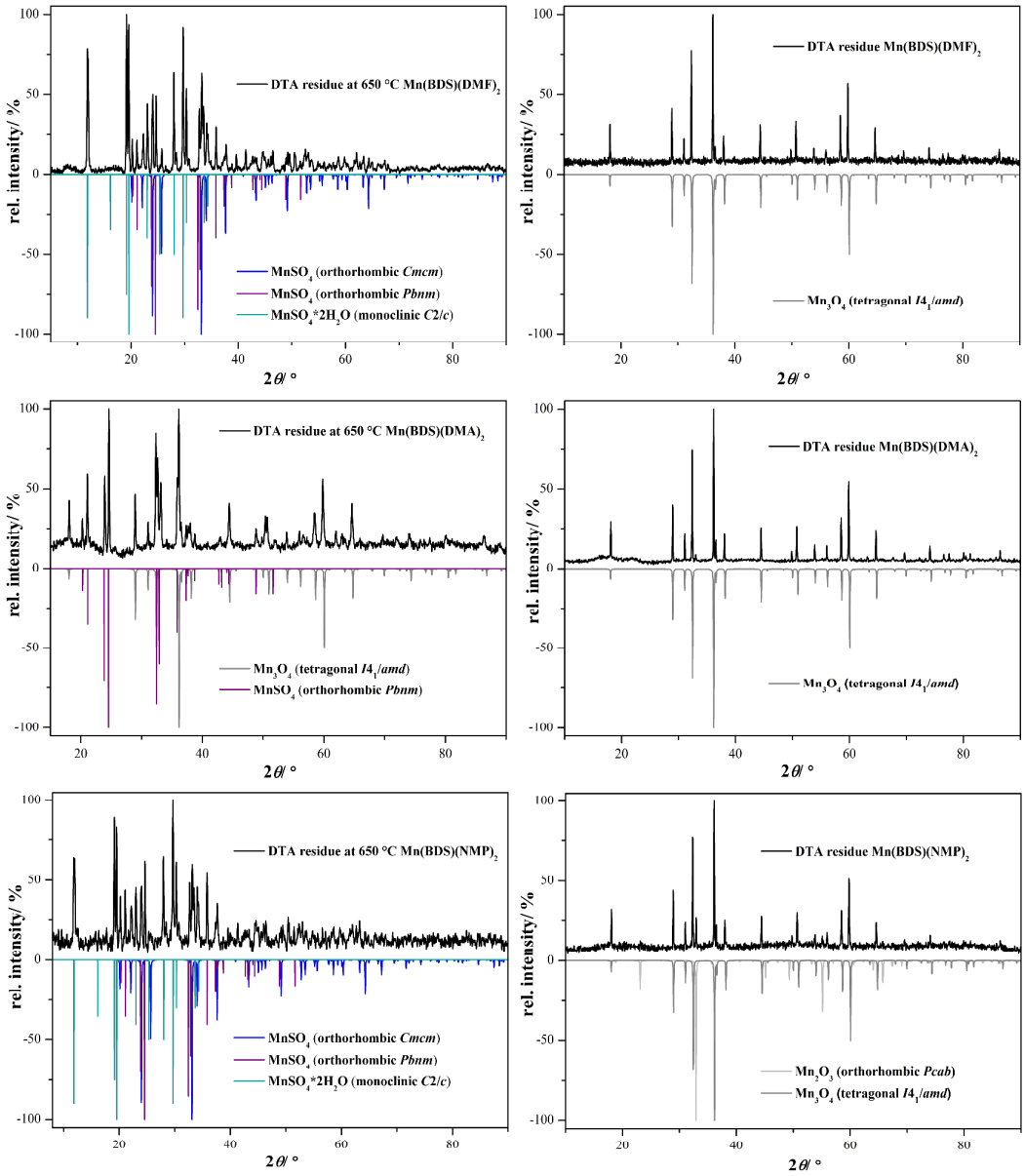

Figure 10. Powder patterns of the intermediate (left) and final product (right) of **III** (on top), **IV** (middle) and **V** (at bottom).

Table 3 Thermal decomposition data of the benzenedisulfonates **III**, **IV**, and **V**

Mn(BDS)(DMF)$_2$						
Stage	T_{onset}/ °C	T_{end}/ °C	T_{max}/ °C	Mass loss obsd./ %	Mass loss calcd./ %	elimination/ decomposition
I	190	245	230	34	33	loss of two equiv. of DMF
II	516	607	577; 592	33	32	decomposition to $MnSO_4$ (calcd. 34%)
III	860	906	895	17	17	decomposition to Mn_3O_4 (calcd. 17%)
∑				84	82	

			$Mn(BDS)(NMP)_2$			
I	110	220	135; 204	34	40	loss of two equiv. of NMP
II	525	560	540	39	40	decomposition to $MnSO_4$ (calcd. 31 %)
III	775	896	890	9	-	decomposition to Mn_2O_3 and $9Mn_3O_4$ (calcd. 16%)
∑				82	84	
			$Mn(BDS)(DMA)_2$			
I	50	195	68; 135; 180	34	37	loss of two equiv. of DMA
II	508	593	547	31	-	decomposition to Mn_3O_4 and $MnSO_4$
III	868	904	895	20	-	decomposition to Mn_3O_4 (calcd. 16%)
∑				85	84	

Magnetic Properties of $[NH_2(CH_3)_2]_2\{Mn(B4S)(DMF)_2\}$

The temperature dependent magnetic susceptibility and inverse magnetic susceptibility data (χ and χ^{-1}) are depicted in Figure 11 (top). The inverse magnetic susceptibility shows linear variation with temperature, indicating Curie-Weiss behavior [$\chi = C / (T - \theta_P)$] over the whole temperature range. A fit of the data set resulted in an effective magnetic moment of 5.19(1) μ_B / Mn atom and a Weiss constant of $\theta_P = -1.9(5)$ K, indicating minute antiferromagnetic interactions in the paramagnetic domain. The effective magnetic moment is in between the values for a Mn^{2+}(h.s.) ion ($\mu_{theo} = 5.92\ \mu_B$) and a Mn^{3+}(h.s.) ion ($\mu_{theo} = 4.90\ \mu_B$).[29] From crystal chemical considerations a Mn^{2+}-ion in high spin configuration is to be expected.

The 100 Oe measurement in *zero-field-cooled/field-cooled* mode (inset of Figure 11; center) reveals a trace amount of a ferromagnetic impurity $T_C = 32.5(5)$ K. This is consistent with the ferromagnetic ordering temperature of $MnCO_3$ ($T_C = 32.2$ K).[30] The ZFC/FC measurement was repeated with a magnetic flux density of 500 Oe in order to saturate the ferromagnetic $MnCO_3$ Impurity (Figure 12; center) in order to show the extrinsic nature of this anomaly. The $MnCO_3$ impurity obviously remains from the synthesis which starts from $MnCO_3$ as the manganese source.

Figure 11 (bottom) shows the magnetization isotherms of the $[NH_2(CH_3)_2]_2\{Mn(B4S)(DMF)_2\}$ sample measured at 5, 10, 25 and 50 K with magnetic flux densities up to 80 kOe. The 5 K isotherm exhibits pronounced curvature without showing any indication of a magnetic ordering phenomenon, the curvature of the 10 K isotherm is less pronounced and the 25 and 50 K isotherms show linear dependence of temperature as is expected for a paramagnetic material.

Taking the trace amount of $MnCO_3$ into account, one can assume the compound to contain Mn^{2+} ions in high spin configuration. No magnetic ordering phenomenon was evident within the investigated temperature range.

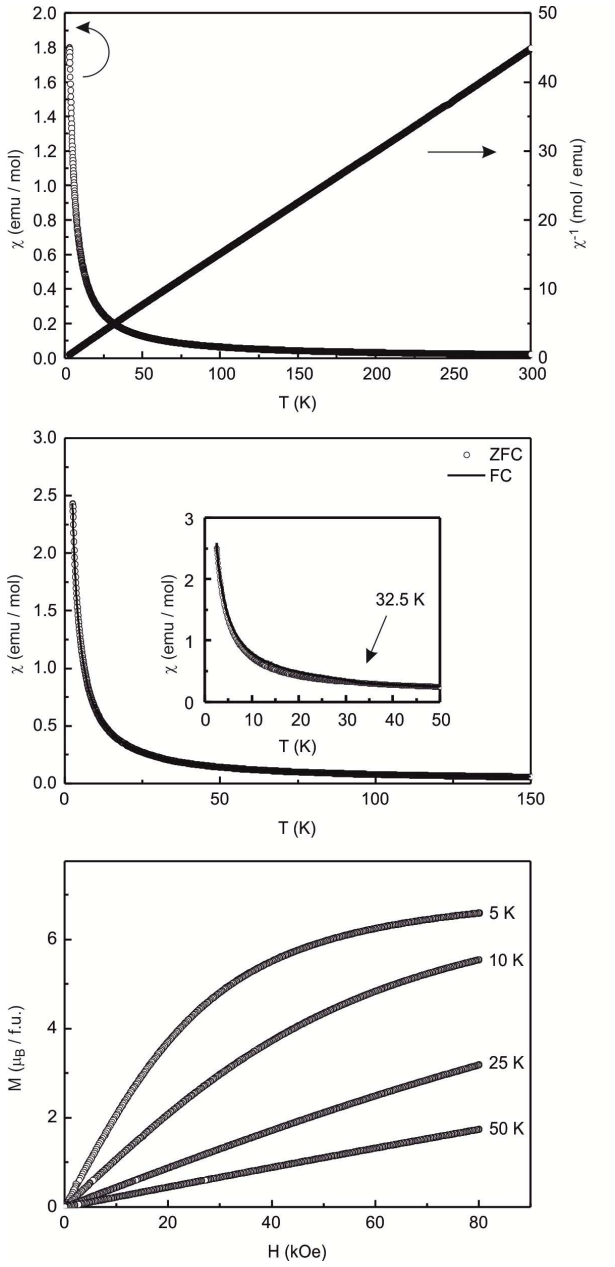

Figure 11. Magnetic behavior of $[NH_2(CH_3)_2]_2\{Mn(B4S)(DMF)_2\}$. The temperature dependent magnetic susceptibility and inverse magnetic susceptibility (upper part) reveals the paramagnetic behaviour of the compound. In *zero-field-cooled*/*field-cooled* measurement mode (middle) a small amount of a ferromagnetic impurity ($MnCO_3$) can be identified. The magnetization isotherms (bottom) gave no hint of a magnetic ordering phenomenon.

Conclusion

In the course of our investigations on the preparation of novel polysulfonic acids and their use in the synthesis of polysulfonates we have obtained five manganese polysulfonates based on the acids H_4B4S (1,2,4,5-benzenetetrasulfonic acid) and H_2BDS (1,4-benzenedisulfonic acid). The compounds were prepared by solvothermal reactions at elevated temperatures. While the tetrasulfonates exhibit unique anionic chains according to $_\infty^1\{Mn(B4S)_{2/2}(L)_2\}^{2-}$ (L = DMF, NMP) the disulfonates show layer type structures. For both kind

of compound thermoanalytical measurements show that the sulfonates have exceptionally high decomposition temperatures, especially when compared to related polycarboxylates.[31] Further investigations shall now elucidate the structures of the solvent free compounds in order to investigate if they are porous MOF type materials. The final decomposition products are Mn_3O_4 and Mn_2O_3. For the chain type tetrasulfonate $[NH_2(CH_3)_2]_2\{Mn(B4S)(DMF)_2\}$ also magneto chemical investigations have been performed proving the ferromagnetic behavior of the compound. Magnetic coupling, however, is not observed. The results presented show that polysulfonates are a highly interesting class of compounds that need further investigation. The fundament for these investigations is the development of preparative routes for polysulfonic acids and thus the strength of this project is the combination of expertises from organic and inorganic chemistry.

Acknowledgement

The authors thank Dipl.-Chem. Wolfgang Saak and Dr. Marc Schmidtmann for the collection of the X-ray data, and Florian Behler for the measurements of the IR spectra. Financial support by the Deutsche Forschungsgemeinschaft is also gratefully acknowledged.

Supporting Information

Crystallographic information files (cif) containing the complete crystallographic data are available as supporting information and can also be obtained from The Cambridge Crystallographic Data Centre via www.ccdc.cam.ac.uk/data_request/cif , or by emailing data_request@ccdc.cam.ac.uk, or by contacting The Cambridge Crystallographic Data Centre, 12, Union Road, Cambridge CB2 1EZ, UK; fax: +44 1223 336033 on quoting the deposition number given in Table 1 and Table 2.

References

[1] a) C. Janiak, *Dalton Trans*., 2003, 2781-2804; b) A. K. Cheetham, C. N. R. Rao and R. K. Feller, *Chem. Commun.,* 2006, 4780-4795.

[2] C. Janiak, J. K. Vieth, *New J. Chem.,* 2010, *34*, 2366-2388.

[3] a) H. Li, M. Eddaoudi, M. O'Keeffe, O. M. Yaghi, *Nature,* 1999, *402*, 276-279; b) U. Mueller, M. Schubert, F. Teich, H. Puetter, K. Schierle-Arndt, J. Pastre, *J. Mater. Chem.,* 2006, *16*, 626-636; c) S. Bauer, N. Stock, *Chem. unserer Zeit,* 2008, *42*, 12-19.

[4] a) J.-M. Shi, W. Xu, Q.-Y. Liu, F.-L. Liu, Z.-L. Huang, H. Lei, W.-T. Yu, Q. Fang, *Chem. Comm*., 2002, 756-757; b) G.-F. Liu, Z.-P. Qiao, H.-Z. Wang, X.-M. Chen, G. Yang, *New J. Chem*., 2002, *26*, 791-795; c) T. M. Reineke, M. Eddaoudi, M. Fehr, D. Kelley, O. M. Yaghi, *J. Am. Chem. Soc*., 1999, *121*, 1651-1657; d) Y. Zhu, Z. Sun, Y. Zhao, J. Zhang, X. Lu, N. Zhang, L. Liu, F. Tong, *New J. Chem*., 2009, *33*, 119-124; e) N. Kerbellec, L. Catala, C. Daiguebonne, A. Gloter, O. Stephan, J.-C. Bünzli, O. Guillou, T. Mallah, *New J. Chem*., 2008, *32*, 584-587; f) X. Yang, J. H. Rivers, W. J. McCarty, M. Wiester, R. A. Jones, *New J. Chem*., 2008, *32*, 790-793.

[5] M. D. Allendorf, C. A. Bauer, R. K. Bhakta, R. J. T. Houk, *Chem. Soc. Rev.,* 2009, *38*, 1330-1352.

[6] a) J. A. Real, E. Andres, M. C. Munoz, M. Julve, T. Granier, A. Bousseksou, F. Varret, *Science,* 1995, *268*, 265-267; b) L. G. Beauvais, M. P. Shores and J. R. Long, *J. Am. Chem. Soc.,* 2000, *122*, 2763-2772.

[7] a) H. A. Habib, J. Sanchiz, C. Janiak, *Dalton Trans*., 2008, 1734-1744; b) D. Maspoch, D. Ruiz-Molina, J. Veciana, *Chem. Soc. Rev*., 2007, *36*, 770-818; c) M. Kurmoo, *Chem. Soc. Rev*., 2009, *38*, 1353-1379; d) J. Larionova, Y. Guari, C. Sangregorio, C. Guérin, *New J. Chem*., 2009, *33*, 1177-1190.

[8] a) L. J. Murray, M. Dincă, J. R. Long, *Chem. Soc. Rev*., 2009, *38*, 1294-1314; b) J. L. C. Rowsell, O. M. Yaghi, *Angew. Chem., Int. Ed*., 2005, *44*, 4670-4679; c) J.-R. Li, R. J. Kuppler, H.-C. Zhou, *Chem. Soc. Rev*., 2009, *38*, 1477-1504; d) C.-J. Li, Z.-j. Lin, M.-X. Peng, J.-D. Leng, M.-M. Yang, M.-L. Tong, *Chem. Commun*., 2008, 6348-6350; e) S. S. Iremonger, P. D. Southon, C. J. Kepert, *Dalton Trans*., 2008, 6103-6105; f) S. Ma, D. Sun, M. Ambrogio, J. A. Fillinger, S. Parkin, H. C. Zhou, *J. Am. Chem. Soc*., 2007, *129*, 1858-1859; g) S. Ma, H.-C. Zhou, *Chem. Commun*., 2010, *46*, 44-53.

[9] Z. Hulvey, E. H. L. Falcao, J. Echert, A. K. Cheetham, *J. Mater. Chem.,* 2009, *19*, 4307-4309.

[10] a) S. Kitagawa, R. Kitaura, S. Noro, *Angew. Chem.,* 2004, *116*, 2388-2430; b) G. Férey, *Chem. Mater*., 2001, *13*, 3084-3098; c) J. L. C. Rowsell, O. M. Yaghi, *Microporous Mesoporous Mater.,* 2004, *73*, 3-14.

[11] a) B. D. Chandler, G. D. Enright, K. A. Udachin, S. Pawsey, J. A. Ripmeester, D. T. Cramb, G. K. H. Shimizu, *Nat. Mater.,* 2008, *7*, 229-235; b) G. K. H. Shimizu, R. Vaidhyanathan, J. M. Taylor, *Chem. Soc. Rev.,* 2009, *38*, 1430-1449; c) G. B. Deacon, A. Gitlits, G. Zelesny, D. Stellfeldt, G. Meyer, *Z. Anorg. Allg. Chem.,* 1999, *625*, 764-772; d) G. B. Deacon, R. Harika, P. C. Junk, B. W. Skelton, A. H. White, *New J. Chem.,* 2007, *31*, 634-645; e) D. J. Hoffart, S. A. Dalrymple, G. K. H. Shimizu, *Inorg. Chem.,* 2005, *44*, 8868-8875; f) V. Videnova-Adrabinska, *Coord. Chem. Rev.,* 2007, *251*, 1987-2016.

[12] a) K. T. Holman, A. M. Pivovar, J. A. Swift, M. D. Ward, *Acc. Chem. Res.,* 2001, *34*, 107-118; b) K. T. Holman, S. M. Martin, D. P. Parker, M. D. Ward, *J. Am. Chem. Soc.,* 2001, *123,* 4421-4431; c) M. J. Horner, K. T. Holman, M. D. Ward, *J. Am. Chem. Soc.,* 2007, *129*, 14640-14660; d) V. A. Russell, C. C. Evans, W. Li, M. D. Ward, *Science,* 1997, *276*, 575-579; e) J. A. Swift, A. M. Pivovar, A. M. Reynolds, *J. Am. Chem. Soc.,* 1998, *24*, 5887-5894; f) J. A. Swift, A. M. Reynolds, M. D. Ward, *Chem. Mater*., 1998, *10*, 4159-4168.

[13] A. Mietrach, T. W. T. Muesmann, J. Christoffers, M. S. Wickleder, *Eur. J. Inorg. Chem.,* 2009,

5328-5334.

[14] T. W. T. Muesmann, A. Mietrach, J. Christoffers, M. S. Wickleder, *Z. Anorg. Allg. Chem.,* 2010, *636*, 1307-131.

[15] a) A. Mietrach, T. W. T. Muesmann, C. Zilinski, J. Christoffers, M. S. Wickleder, *Z. Anorg. Allg. Chem*., 2011, *637*, 195-200; b) T. W. T. Muesmann, C. Zitzer, A. Mietrach, T. Klüner, J. Christoffers, M. S. Wickleder, *Dalton Trans.,* 2011, *40*, 3128-3141; c) T. W. T. Muesmann, C. Zitzer, M. S. Wickleder, J. Christoffers, *Inorg. Chim. Acta,* 2011, *369*, 45-48.

[16] BrukerOptik GmbH, *OPUS 6.5*, Germany, 2009.

[17] a) G. M. Sheldrick, *Acta Crystallogr.,* 2008, *A64*, 112-122; b) X-*RED 1.22*; Stoe & Cie: Darmstadt, Germany, 2001; c) *X-SHAPE 1.06f*. Stoe & Cie: Darmstadt, Germany, 1999.

[18] *Star^e V 9.3*; Mettler-Toledo GmbH: Schwerzenbach, Switzerland, 2009.

[19] *WinXPOW 2007*; Stoe & Cie: Darmstadt, Germany, 2006.

[20] G. A. Jeffrey*, An Introduction to Hydrogen Bonding*, Oxford University Press, New York, 1997.

[21] O.V. Dolomanov, L.J. Bourhis, R.J. Gildea, J.A.K. Howard, H. Puschmann, OLEX2: *J. Appl. Crystallogr.,* 2009, *42*, 339-341.

[22] A. Kirfel, G. Will, *High Temp. High Press.,* 1974, *6*, 525-527.

[23] G. Aminoff, *Z. Kristallogr.Kristallgeo.,* 1927, *64*, 475-490.

[24] Yu.D. Kondrashev, A.I. Zaslavskii, *Golden Book of Phase Transitions*, Wroclaw, 2002, 1, 1-123.

[25] S. Geller, *Acta Crystallogr*., 1971, *B27*, 821-828.

[26] G. Will, *Acta Crystallogr*., 1965, *19*, 854-857.

[27] F. Golinska, A. Lodzinska, F. Rozploch, *Pol. J. Chem*., 1984, *58*, 31-39.

[28] PANalytical, *High Score Plus V 3.0d*, B. V., Almelo, Netherlands, 2011.

[29] H. Lueken, *Magnetochemie*, B.G. Teubner, Stuttgart, 1999.

[30] a) I. Maartense, *Phys. Rev.,* 1969, *188*, 924-930; b) A. Kosterov, T. Frederichs, T. von Dobeneck, *Phys. Earth Planet. Int.,* 2006,*154*, 234-242.

[31] a) L.-F. Song, C.-H. Jiang, C.-L. Jiao, J. Zhang, L.-X. Sun, F. Xu, Q.-Z. Jiao, Y.-H. Xing, Y. Du, Z. Cao, F.-L. Huang, *J. Therm. Anal. Calorim.* 2010,, *102*, 1161-1166; b) R.-Q. Zhong, R.-Q. Zou, M. Du, T. Yamada, G. Maruta, S. Takeda, J. Li, Q. Xu, *CrystEngComm,* 2010, *12*, 677-681; c) Y. Liu, H. Li, Y. Han, X. Lv, H. Hou, Y. Fan, *Cryst. Growth Des*., 2012, *12*, 3505-3513.

Table 4 Crystallographic Data of $[NH_2(CH_3)_2]_2\{Mn(B4S)(DMF)_2\}$ and $[HNMP]_2\{Mn(B4S)(NMP)_2\}$ and their determination

	$[NH_2(CH_3)_2]_2\{Mn(B4S)(DMF)_2\}$	$[HNMP]_2\{Mn(B4S)(NMP)_2\}$
lattice parameters	a = 942.02(5) pm	a = 931.70(7) pm
	b = 1684.86(6) pm	b = 1049.19(7) pm
	c = 918.45(5) pm	c = 1944.87(12) pm
	β = 97.746(6)°	β = 113.529(3)°
density (calculated g cm^{-3})	1.58	1.62
cell volume	1444.4(1) Å³	1743.1(2) Å³
no. of formula units	2	2
cryst. syst.	monoclinic	monoclinic
space group	$P2_1/c$ (no.14)	$P2_1/c$ (no.14)
measuring device	Stoe IPDS I	Bruker APEX II
radiation	Mo-K_α, λ = 71.07 pm	Mo-K_α, λ = 71.07 pm
temp.	296 K	120 K
absorption correction	numerical	numerical
μ	8.2 cm^{-1}	7.0 cm^{-1}
measured reflections	22160	77638
unique reflections	3560	5757
with $I_o > 2\sigma(I_o)$	2330	4016
R_{int}; R_σ	0.0668; 0.0514	0.0512; 0.0384
GOF (all data)	0.870	1.029
$R1$; $wR2$ ($I_o > 2\sigma(I_o)$)	0.0357; 0.0771	0.0501; 0.1310
$R1$; $wR2$ (all data)	0.0643; 0.0837	0.0818; 0.1484
max./min. electron density	0.62/-0.26 e/Å³	1.10/-0.47 e/Å³
CCDC number	951310	959360

Table 5 Crystallographic Data of $Mn(BDS)(DMF)_2$, $Mn(BDS)(DMA)_2$, and $Mn(BDS)(NMP)_2$

	$Mn(BDS)(DMF)_2$	$Mn(BDS)(DMA)_2$	$Mn(BDS)(NMP)_2$
lattice parameters	a = 514.30(7) pm	a = 936.00(4) pm	a = 962.97(3) pm
	b = 926.20(12) pm	b = 984.94(4) pm	b = 976.76(3) pm
	c = 940.20(13) pm	c = 1034.75(5) pm	c = 1034.23(3) pm
	α = 93.552(8)°	α = 81.606(2)°	α = 89.3710(10)°
	β = 99.993(7)°	β = 88.941(2)°	β = 78.8390(10)°
	γ = 99.237(7)°	γ = 82.364(2)°	γ = 87.604(2)°
density (calculated g cm^{-3})	1.68	1.65	1.71
cell volume	433.48(10) Å³	935.35(7) Å³	953.55(5) Å³
no. of formula units	1	2	2
cryst. syst.	triclinic	triclinic	triclinic
space group	P-1 (Nr. 2)	P-1 (Nr. 2)	P-1 (Nr. 2)
measuring device	Bruker APEX II	Bruker APEX II	Bruker APEX II
radiation	Mo-K_α, λ = 71.07 pm	Mo-K_α, λ = 71.07 pm	Mo-K_α, λ = 71.07 pm
temp.	120 K	120 K	120 K
absorption correction	numerical	numerical	numerical
μ	10.5 cm^{-1}	9.8 cm^{-1}	9.6 cm^{-1}

measured reflections	9686	25447	46913
unique reflections	3443	8169	11970
with $I_o > 2\sigma(I_o)$	2587	6324	9790
R_{int}; R_σ	0.0393; 0.0520	0.0726; 0.0502	0.0315; 0.0237
GOF (all data)	0.956	1.045	1.021
$R1$; $wR2$ ($I_o > 2\sigma(I_o)$)	0.0290; 0.0637	0.0348; 0.0939	0.0243; 0.0713
$R1$; $wR2$ (all data)	0.0462; 0.0670	0.0504; 0.1002	0.0314; 0.0733
max./min. electron density	0.46/-0.40 e/Å³	1.09/-0.59 e/Å³	0.59/-0.47 e/Å³
CCDC number	951313	951315	951316

Table 6 Selected Distances (pm) and Angles (deg.) for $[NH_2(CH_3)_2]_2\{Mn(B4S)(DMF)_2\}$ and $[HNMP]_2\{Mn(B4S)(NMP)_2\}$.

	$[NH_2(CH_3)_2]_2\{Mn(B4S)(DMF)_2\}$				$[HNMP]_2\{Mn(B4S)(NMP)_2\}$			
$[MnO_6]$	Mn1	-O1(2x)		217.1(2)	Mn1	-O1(2x)		215.7(2)
		-O11(2x)		216.4(2)		-O11(2x)		219.1(4)
		-O14(2x)		215.4(2)		-O14(2x)		218.3(3)
	O1-	Mn1	-O11	90.47(7)	O1-	Mn1	-O11	89.4(1)
	O1-	Mn1	-O14	89.79(7)	O1-	Mn1	-O14	88.4(1)
	O11-	Mn1	-O14	86.11(6)	O11-	Mn1	-O14	96.3(1)
$[SO_3]$	S1	-O11		146.3(2)	S1	-O11		146.1(4)
		-O12		143.4(2)		-O12		144.2(4)
		-O13		144.8(2)		-O13		144.2(4)
		-C1		179.4(2)		-C1		180.2(2)
	S2	-O14		145.6(2)	S2	-O14		141.9(3)
		-O15		143.0(2)		-O15		149.3(3)
		-O16		144.3(2)		-O16		143.3(4)
		-C2		181.0(2)		-C2		179.5(2)
	O11-	S1	-O12	113.8(1)	O11-	S1	-O12	112.9(2)
	O11-	S1	-O13	110.4(1)	O11-	S1	-O13	111.6(2)
	O12-	S1	-O13	114.1(1)	O12-	S1	-O13	114.6(2)
	O11-	S1	-C1	104.9(1)	O11-	S1	-C1	105.4(2)
	O12-	S1	-C1	107.1(1)	O12-	S1	-C1	106.8(2)
	O13-	S1	-C1	105.7(1)	O13-	S1	-C1	104.7(2)
	O14-	S2	-O15	113.2(1)	O14-	S2	-O15	111.2(2)
	O14-	S2	-O16	111.3(1)	O14-	S2	-O16	115.4(2)
	O15-	S2	-O16	113.2(1)	O15-	S2	-O16	110.1(2)
	O14-	S2	-C2	107.5(1)	O14-	S2	-C2	107.9(1)
	O15-	S2	-C2	105.1(1)	O15-	S2	-C2	105.3(1)
	O16-	S2	-C2	105.9(1)	O16-	S2	-C2	106.2(2)

Table 7 Selected Distances (pm) and Angles (deg.) for $Mn(BDS)(DMF)_2$, $Mn(BDS)(DMA)_2$, and $Mn(BDS)(NMP)_2$

	$Mn(BDS)(DMF)_2$				$Mn(BDS)(DMA)_2$				$Mn(BDS)(NMP)_2$			
$[MnO_6]$	Mn1	-O1 (2x)		215.09(9)	Mn1	-O1		213.4(1)	Mn1	-O1		213.07(5)
		-O11 (2x)		218.41(9)		-O2		211.9(1)		-O2		213.51(5)
		-O12 (2x)		214.49(9)		-O11		219.6(1)		-O11		219.19(5)
						-O12		219.0(1)		-O12		219.12(4)
						-O14		217.7(1)		-O14		217.25(5)
						-O15		219.4(1)		-O15		218.89(5)
	O1-	Mn1	-O11	91.86(4)	O1-	Mn1	-O2	174.94(5)	O1-	Mn1	-O2	172.86(2)
	O1-	Mn1	-O12	93.09(4)	O1-	Mn1	-O11	91.07(4)	O1-	Mn1	-O11	87.52(2)
	O11-	Mn1	-O12	90.16(4)	O1-	Mn1	-O12	89.16(4)	O1-	Mn1	-O12	90.10(2)
					O1-	Mn1	-O14	90.04(5)	O1-	Mn1	-O14	91.12(2)
					O1-	Mn1	-O15	85.67(5)	O1-	Mn1	-O15	87.32(2)
					O2-	Mn1	-O11	92.06(5)	O2-	Mn1	-O11	91.18(2)
					O2-	Mn1	-O12	86.94(5)	O2-	Mn1	-O12	96.91(2)
					O2-	Mn1	-O14	94.04(5)	O2-	Mn1	-O14	90.43(2)
					O2-	Mn1	-O15	91.21(5)	O2-	Mn1	-O15	85.70(2)
					O11-	Mn1	-O12	88.75(4)	O11-	Mn1	-O12	89.37(2)
					O11-	Mn1	-O14	87.99(5)	O11-	Mn1	-O14	177.52(2)
					O11-	Mn1	-O15	176.73(4)	O11-	Mn1	-O15	91.74(2)
					O12-	Mn1	-O14	176.63(5)	O12-	Mn1	-O14	88.56(2)
					O12-	Mn1	-O15	91.36(5)	O12-	Mn1	-O15	177.15(2)
					O14-	Mn1	-O15	91.84(5)	O14-	Mn1	-O15	90.26(2)
$[SO_3]$	S1	-O11		1.46.2(1)	S1	-O11		146.2(1)	S1	-O11		146.19(5)
		-O12		1.45.1(1)		-O12		145.9(1)		-O12		146.13(5)
		-O13		1.44.2(1)		-O13		144.4(1)		-O13		144.65(5)
		-C1		1.76.8(1)		-C1		177.8(1)		-C1		177.21(6)
					S2	-O14		145.4(1)	S2	-O14		146.02(5)
						-O15		145.0(1)		-O15		145.89(5)
						-O16		144.1(1)		-O16		144.25(6)
						-C4		177.5(1)		-C4		177.94(6)
	O11-	S1	-O12	112.07(5)	O11-	S1	-O12	112.51(7)	O11-	S1	-O12	112.85(3)

O11-	S1	-O13	112.01(6)	O11-	S1	-O13	112.61(7)	O11-	S1	-O13	112.33(3)
O12-	S1	-O13	114.01(6)	O12-	S1	-O13	114.65(7)	O12-	S1	-O13	113.89(3)
O11-	S1	-C1	106.41(6)	O11-	S1	-C1	105.84(6)	O11-	S1	-C1	106.18(3)
O12-	S1	-C1	105.02(6)	O12-	S1	-C1	104.07(6)	O12-	S1	-C1	105.07(3)
O13-	S1	-C1	106.61(6)	O13-	S1	-C1	106.15(7)	O13-	S1	-C1	105.64(3)
				O14-	S2	-O15	113.02(8)	O14-	S2	-O15	112.84(3)
				O14-	S2	-O16	113.84(8)	O14-	S2	-O16	111.95(3)
				O15-	S2	-O16	112.37(8)	O15-	S2	-O16	114.61(3)
				O14-	S2	-C4	104.89(7)	O14-	S2	-C4	106.48(3)
				O15-	S2	-C4	105.98(7)	O15-	S2	-C4	104.19(3)
				O16-	S2	-C4	105.84(7)	O16-	S2	-C4	105.85(3)